J|A|C|S ARTICLES

Published on Web 04/20/2009

Probing the Structure and Charge State of Glutathione-Capped $Au_{25}(SG)_{18}$ Clusters by NMR and Mass Spectrometry

Zhikun Wu, Chakicherla Gayathri, Roberto R. Gil, and Rongchao Jin*

Department of Chemistry, Carnegie Mellon University, Pittsburgh, Pennsylvania 15213

Received January 23, 2009; E-mail: rongchao@andrew.cmu.edu

Abstract: Despite the recent crystallographic determination of the crystal structure of $Au_{25}(SCH_2CH_2Ph)_{18}$ clusters, the question—whether all thiolate-capped, 25-atom gold clusters adopt the same structure, regardless of the types of thiols (e.g., long-chain alkylthiols, aromatic thiols, or other functionalized ones)—still remains unanswered. To crystallize long-chain or bulky ligand (e.g., glutathione)-capped $Au_{25}(SR)_{18}$ clusters has proven to be difficult due to the major amorphousness caused by such ligands; therefore, one needs to seek other strategies to probe the structural information of such gold clusters. Herein, we report a strategy to probe the Au_{25} core structure and surface thiolate ligand distribution by means of NMR in combination with mass spectrometry. We use glutathione-capped $Au_{25}(SG)_{18}$ clusters as an example to demonstrate the utility of this strategy. One-dimensional (1D) and two-dimensional (2D) correlation NMR spectroscopic investigation of $Au_{25}(SG)_{18}$ reveals fine spectral features that explicitly indicate two types of surface binding modes of thiolates, which is consistent with the ligand distribution in the $Au_{25}(SCH_2CH_2Ph)_{18}$ cluster. Laser desorption ionization (LDI) mass spectrometry analysis shows that $Au_{25}(SG)_{18}$ exhibits an identical ionization and core fragmentation pattern with phenylethylthiolate-capped Au_{25} clusters. The charge state of the native $Au_{25}(SG)_{18}$ clusters was determined to be -1 by comparing their optical spectrum with those of $[Au_{25}(SCH_2CH_2Ph)_{18}]^q$ of different charge states ($q = -1, 0$). Taken together, our results led to the conclusion that glutathione-capped $Au_{25}(SG)_{18}$ clusters indeed adopt the same structure as that of $Au_{25}(SCH_2CH_2Ph)_{18}$. This conclusion is also valid for other types of thiolate-capped Au_{25} clusters, including hexyl- and dodecylthiolates. Interestingly, the chiral optical responses (e.g., circular dichroism (CD) signals in the visible wavelength region) from the $Au_{25}(SG)_{18}$ clusters seem to be imparted by the chiral glutathione ligands because no similar CD signals were observed in $Au_{25}(SCH_2CH_2Ph)_{18}$.

1. Introduction

When the size of gold nanoparticles becomes smaller than ~2 nm (core diameter), they start to exhibit discrete electronic structure and distinct HOMO—LUMO transition in optical absorption,[1−5] intrinsic magnetism,[6,7] enhanced photoluminescence,[8−10] discrete charge transport, and redox properties.[11−18] These unique properties of gold nanoclusters are fundamentally different from those of their larger counterparts—gold nanocrystals. The latter possess quasicontinuous electronic energy band structure, and their optical properties are dominated by surface plasmons.[19,20] Owing to the interesting physiochemical properties of gold nanoclusters, this type of material has attracted significant research interest in both fundamental science studies and technological exploration of their potential applications in

(1) Zhu, M.; Aikens, C. M.; Hollander, F. J.; Schatz, G. C.; Jin, R. *J. Am. Chem. Soc.* **2008**, *130*, 5883.
(2) Aikens, C. M. *J. Phys. Chem. C* **2008**, *112*, 19797.
(3) Shichibu, Y.; Negishi, Y.; Watanabe, T.; Chaki, N. K.; Kawaguchi, H.; Tsukuda, T. *J. Phys. Chem. C* **2007**, *111*, 7845.
(4) Nobusada, K.; Iwasa, T. *J. Phys. Chem. C* **2007**, *111*, 14279.
(5) Wyrwas, R. B.; Alvarez, M. M.; Khoury, J. T.; Price, R. C.; Schaaff, T. G.; Whetten, R. L. *Eur. Phys. J. D* **2007**, *43*, 91.
(6) Zhu, M.; Aikens, C. M.; Hendrich, M. P.; Gupta, R.; Qian, H.; Schatz, G. C.; Jin, R. *J. Am. Chem. Soc.* **2009**, *131*, 2490.
(7) Negishi, Y.; Tsunoyama, H.; Suzuki, M.; Kawamura, N.; Matsushita, M. M.; Maruyama, K.; Sugawara, T.; Yokoyama, T.; Tsukuda, T. *J. Am. Chem. Soc.* **2006**, *128*, 12034.
(8) (a) Bigioni, T. P.; Whetten, R. L.; Dag, Ö. *J. Phys. Chem. B* **2000**, *104*, 6983. (b) Link, S.; Beeby, A.; FitzGerald, S.; El-Sayed, M. A.; Schaaff, T. G.; Whetten, R. L. *J. Phys. Chem. B* **2002**, *106*, 3410. (c) Wang, G.; Huang, T.; Murray, R. W.; Menard, L.; Nuzzo, R. G. *J. Am. Chem. Soc.* **2005**, *127*, 812.
(9) (a) Zheng, J.; Petty, J. T.; Dickson, R. M. *J. Am. Chem. Soc.* **2003**, *125*, 7780. (b) Bao, Y.; Zhong, C.; Vu, D. M.; Temirov, J. P.; Dyer, R. B.; Martinez, J. S. *J. Phys. Chem. C* **2007**, *111*, 12194. (c) Xie, J.; Zheng, Y.; Ying, J. Y. *J. Am. Chem. Soc.* **2009**, *131*, 888. (d) Sakamoto, M.; Tachikawa, T.; Fujitsuka, M.; Majima, T. *J. Am. Chem. Soc.* **2009**, *131*, 6.
(10) (a) Lin, C.-A. J.; Yang, T.-Y.; Lee, C.-H.; Huang, S. H.; Sperling, R. A.; Zanella, M.; Li, J. K.; Shen, J.-L.; Wang, H.-H.; Yeh, H.-I.; Parak, W. J.; Chang, W. H. *ACS Nano* **2009**, *3*, 395. (b) Liu, X.; Li, C.; Xu, J.; Lv, J.; Zhu, M.; Guo, Y.; Cui, S.; Liu, H.; Wang, S.; Li, Y. *J. Phys. Chem. C* **2008**, *112*, 10778.
(11) Ingram, R. S.; Hostetler, M. J.; Murray, R. W.; Schaaff, T. G.; Khoury, J. T.; Whetten, R. L.; Bigioni, T. P.; Guthrie, D. K.; First, P. N. *J. Am. Chem. Soc.* **1997**, *119*, 9279.
(12) (a) Chen, S. W.; Ingram, R. S.; Hostetler, M. J.; Pietron, J. J.; Murray, R. W.; Schaaff, T. G.; Khoury, J. T.; Alvarez, M. M.; Whetten, R. L. *Science* **1998**, *280*, 2098. (b) Georganopoulou, D. G.; Mirkin, M. V.; Murray, R. W. *Nano Lett.* **2004**, *4*, 1763.
(13) (a) Chen, S. *J. Phys. Chem. B.* **2000**, *104*, 663. (b) Yang, Y.; Chen, S. *Nano Lett.* **2003**, *3*, 75.
(14) (a) Quinn, B. M.; Liljeroth, P.; Ruiz, V.; Laaksonen, T.; Kontturi, K. *J. Am. Chem. Soc.* **2003**, *125*, 6644. (b) Toikkanen, O.; Ruiz, V.; Roïnholm, G.; Kalkkinen, N.; Liljeroth, P.; Quinn, B. M. *J. Am. Chem. Soc.* **2008**, *130*, 11049.

a number of fields such as catalysis,[21,22] optics,[23−25] chemical sensing,[26] and biomedicine.[27,28]

The recent advances in nanochemistry have permitted the synthesis of relatively monodisperse thiolate-capped gold nanoclusters[29−36] and others[37,38] with somewhat size control. Among the gold clusters stabilized by various types of thiolates, glutathione (denoted as GSH)-capped gold clusters are perhaps the most extensively studied system.[39−41] Early work was performed by Whetten and co-workers, who reported the first synthesis of an abundant ∼5 kDa (Au_xS_y core mass) Au:SG species.[39a] Recently, a number of size discrete $Au_n(SG)_m$ clusters have been identified by Tsukuda and co-workers by running high-resolution polyacrylamide electrophoresis analysis, including $Au_{10}(SG)_{10}$, $Au_{15}(SG)_{13}$, $Au_{18}(SG)_{14}$, $Au_{22}(SG)_{16}$, $Au_{25}(SG)_{18}$, $Au_{29}(SG)_{20}$, $Au_{33}(SG)_{22}$, and $Au_{39}(SG)_{24}$ clusters.[40] The $Au_{25}(SG)_{18}$ species has been demonstrated to be the most stable one among this series.[40b] However, the crystal structure of $Au_{25}(SG)_{18}$ has not been attained thus far, mainly due to the difficulties encountered in growing high-quality single crystals of such clusters. On the other hand, the crystal structure of a similar Au_{25} thiolate cluster, phenylethylthiolate-capped $Au_{25}(SCH_2CH_2Ph)_{18}$ has recently been reported by Jin and co-workers[1,42] (also independently by Murray and co-workers[43] and theoretically described by Akola et al.[44]). Both the anionic $[Au_{25}(SCH_2CH_2Ph)_{18}]^-$ (counterion: tetraoctylammonium TOA^+)[1,43] and neutral $[Au_{25}(SCH_2CH_2Ph)_{18}]^0$ clusters[42] feature a centered icosahedral Au_{13} kernel encapsulated by an exterior gold shell composed of the remaining 12 gold atoms in six −S−Au−S−Au−S− staples, and the entire particle exhibits a quasi-D_{2h} symmetry but with some distortions;[1] whereas in the charge neutral $[Au_{25}(SCH_2CH_2Ph)_{18}]^0$ cluster, the structural distortions were not observed.[42]

Despite the success in the case of $Au_{25}(SCH_2CH_2Ph)_{18}$, in general, it is still a major challenge to grow single crystals of gold thiolate clusters. Given the unavailability of the crystal structure of $Au_{25}(SG)_{18}$ clusters, it is highly desirable to probe the structure of $Au_{25}(SG)_{18}$ by other means, in particular, to confirm whether its structure is similar to that of $Au_{25}(SCH_2CH_2Ph)_{18}$. This is especially important if further studies of their physical and chemical properties are to be carried out (e.g., surface enhanced Raman scattering,[23] energy transfer between surface-bound chromophores and the Au_{25} core[25b]) and if the full potential of this unique type of clusters is to be fulfilled.

The $Au_{25}(SG)_{18}$ cluster being identical in composition to $Au_{25}(SCH_2CH_2Ph)_{18}$ does not necessarily mean that the same structure as that of $Au_{25}(SCH_2CH_2Ph)_{18}$ is adopted in the $Au_{25}(SG)_{18}$ cluster. In the previous work, several types of Au_{25} core framework have been reported in experiment and theoretically described; among the structures, biicosahedral[3] and two-shell[1,42,43] Au_{25} structures have been crystallographically determined. A few other optimized structures have also been described in theoretical work.[44,45] Given the bulky GSH ligands, it is of particular interest to confirm if the surface strain results

(15) (a) Antonello, S.; Holm, A. H.; Instuli, E.; Maran, F. *J. Am. Chem. Soc.* **2007**, *129*, 9836. (b) Fabris, L.; Antonello, S.; Armelao, L.; Donkers, R. L.; Polo, F.; Toniolo, C.; Maran, F. *J. Am. Chem. Soc.* **2006**, *128*, 326.
(16) Peterson, R. R.; Cliffel, D. E. *Langmuir* **2006**, *22*, 10307.
(17) Kim, J.; Lee, D. *J. Am. Chem. Soc.* **2006**, *128*, 4518.
(18) Nair, A. S.; Kimura, K. *Langmuir* **2009**, *25*, 1750.
(19) (a) Jin, R.; Cao, Y. W.; Hao, E.; Metraux, G. S.; Schatz, G. C.; Mirkin, C. A. *Nature (London)* **2003**, *425*, 487. (b) Jin, R.; Jureller, J. E.; Kim, H. Y.; Scherer, N. F. *J. Am. Chem. Soc.* **2005**, *127*, 12482.
(20) Kelly, K. L.; Coronado, E.; Zhao, L. L.; Schatz, G. C. *J. Phys. Chem. B.* **2003**, *107*, 668.
(21) Chaki, N. K.; Tsunoyama, H.; Negishi, Y.; Sakurai, H.; Tsukuda, T. *J. Phys. Chem. C* **2007**, *111*, 4885.
(22) (a) Maye, M. M.; Luo, J.; Han, L.; Kariuki, N. N.; Zhong, C. J. *Gold Bull.* **2003**, *36*, 75. (b) Chechik, V.; Crooks, R. M. *Langmuir* **1999**, *15*, 6364. (c) Long, C. G.; Gilbertson, J. D.; Vijayaraghavan, G.; Stevenson, K. J.; Pursell, C. J.; Chandler, B. D. *J. Am. Chem. Soc.* **2008**, *130*, 10103. (d) Bonomi, R.; Selvestrel, F.; Lombardo, V.; Sissi, C.; Polizzi, S.; Mancin, F.; Tonellato, U.; Scrimin, P. *J. Am. Chem. Soc.* **2008**, *130*, 15744.
(23) Price, R. C.; Whetten, R. L. *J. Phys. Chem. B* **2006**, *110*, 22166.
(24) (a) Ramakrishna, G.; Varnavski, O.; Kim, J.; Lee, D.; Goodson, T. *J. Am. Chem. Soc.* **2008**, *130*, 5032. (b) Zhang, H.; Zelmon, D. E.; Deng, L.; Liu, H.-K.; Teo, B. K. *J. Am. Chem. Soc.* **2001**, *123*, 11300.
(25) (a) Gu, T.; Whitesell, J. K.; Fox, M. A. *Chem. Mater.* **2003**, *15*, 1358. (b) Muhammed, M. A. H.; Shaw, A. K.; Pal, S. K.; Pradeep, T. *J. Phys. Chem. C* **2008**, *112*, 14324.
(26) (a) Wohltjen, H.; Snow, A. W. *Anal. Chem.* **1998**, *70*, 2856. (b) Rowe, M. P.; Plass, K. E.; Kim, K.; Kurdak, C.; Zellers, E. T; Matzger, A. J. *Chem. Mater.* **2004**, *16*, 3513. (c) Joseph, Y.; Guse, B.; Vossmeyer, T.; Yasuda, A. *J. Phys. Chem. C* **2008**, *112*, 12507.
(27) (a) Hainfeld, J. F.; Liu, W. Q.; Barcena, M. *J. Struct. Biol.* **1999**, *127*, 120. (b) Bowman, M.-C.; Ballard, T. E.; Ackerson, C. J.; Feldheim, D. L.; Margolis, D. M.; Melander, C. *J. Am. Chem. Soc.* **2008**, *130*, 6896.
(28) Ackerson, C. J.; Jadzinsky, P. D.; Jensen, G. J.; Kornberg, R. D. *J. Am. Chem. Soc.* **2006**, *128*, 2635.
(29) (a) Schaaff, T. G.; Shafigullin, M. N.; Khoury, J. T.; Vezmar, I.; Whetten, R. L.; Cullen, W. G.; First, P. N.; Gutierrez-Wing, C.; Ascensio, J.; Jose-Yacaman, M. J. *J. Phys. Chem. B.* **1997**, *101*, 7885. (b) Schaaff, T. G.; Whetten, R. L. *J. Phys. Chem. B* **1999**, *103*, 9394. (c) Price, R. C.; Whetten, R. L. *J. Am. Chem. Soc.* **2005**, *127*, 13750.
(30) (a) Donkers, R. L.; Lee, D.; Murray, R. W. *Langmuir* **2004**, *20*, 1945. (b) Jimenez, V. L.; Georganopoulou, D. G.; White, R. J.; Harper, A. S.; Mills, A. J.; Lee, D.; Murray, R. W. *Langmuir* **2004**, *20*, 6864.
(31) (a) Chaki, N. K.; Negishi, Y.; Tsunoyama, H.; Shichibu, Y.; Tsukuda, T. *J. Am. Chem. Soc.* **2008**, *130*, 8608. (b) Tsunoyama, H.; Nickut, P.; Negishi, Y.; Al-Shamery, K.; Matsumoto, Y.; Tsukuda, T. *J. Phys. Chem. C* **2007**, *111*, 4153.
(32) (a) Zhu, M.; Lanni, E.; Garg, N.; Bier, M. E.; Jin, R. *J. Am. Chem. Soc.* **2008**, *130*, 1138. (b) Jin, R.; Egusa, S.; Scherer, N. F. *J. Am. Chem. Soc.* **2004**, *126*, 9900. (c) Qian, H.; Zhu, M.; Andersen, U. N.; Jin, R. *J. Phys. Chem. A* **2009**, DOI: 10.1021/jp810893w.
(33) Wu, Z.; Suhan, J.; Jin, R. *J. Mater. Chem.* **2009**, *19*, 622.
(34) (a) Kim, J.; Lema, K.; Ukaigwe, M.; Lee, D. *Langmuir* **2007**, *23*, 7853. (b) Wilcoxon, J. P.; Provencio, P. *J. Phys. Chem. B* **2003**, *107*, 12949. (c) Woehrle, G. H.; Warner, M. G.; Hutchison, J. E. *J. Phys. Chem. B.* **2002**, *106*, 9979.
(35) (a) Hussain, I.; Graham, S.; Wang, Z.; Tan, B.; Sherrington, D. C.; Rannard, S. P.; Cooper, A. I.; Brust, M. *J. Am. Chem. Soc.* **2005**, *127*, 16398. (b) Ackerson, C. J.; Jadzinsky, P. D.; Kornberg, R. D. *J. Am. Chem. Soc.* **2005**, *127*, 6550.
(36) (a) Nishida, N.; Yao, H.; Ueda, T.; Sasaki, A.; Kimura, K. *Chem. Mater.* **2007**, *19*, 2831. (b) Gies, A. P.; Hercules, D. M.; Gerdon, A. E.; Cliffel, D. E. *J. Am. Chem. Soc.* **2007**, *129*, 1095.
(37) (a) de Silva, N.; Dahl, L. F. *Inorg. Chem.* **2005**, *44*, 9604. (b) Sevillano, P.; Fuhr, O.; Hampe, O.; Lebedkin, S.; Neiss, C.; Ahlrichs, R.; Fenske, D.; Kappes, M. M. *Eur. J. Inorg. Chem.* **2007**, 5163. (c) Benfield, R. E.; Grandjean, D.; Kroll, M.; Pugin, R.; Sawitowski, T.; Schmid, G. *J. Phys. Chem. B.* **2001**, *105*, 1961. (d) Schulz-Dobrick, M.; Jansen, M. *Eur. J. Inorg. Chem.* **2006**, 4498. (e) Wen, F.; Englert, U.; Gutrath, B.; Simon, U. *Eur. J. Inorg. Chem.* **2008**, 106.
(38) (a) Ott, L. S.; Finke, R. G. *Inorg. Chem.* **2006**, *45*, 8382. (b) Wu, S.; Zeng, H.; Schelly, Z. A. *J. Phys. Chem. B* **2005**, *109*, 18715.
(39) (a) Schaaff, T. G.; Knight, G.; Shafigullin, M. N.; Borkman, R. F.; Whetten, R. L. *J. Phys. Chem. B* **1998**, *102*, 10643. (b) Schaaff, T. G.; Whetten, R. L. *J. Phys. Chem. B* **2000**, *104*, 2630.
(40) (a) Negishi, Y.; Nobusada, K.; Tsukuda, T. *J. Am. Chem. Soc.* **2005**, *127*, 5261. (b) Shichibu, Y.; Negishi, Y.; Tsunoyama, H.; Kanehara, M.; Teranishi, T.; Tsukuda, T. *Small* **2007**, *3*, 835.
(41) Shibu, E. S.; Habeeb Muhammed, M. A.; Tsukuda, T.; Pradeep, T. *J. Phys. Chem. C* **2008**, *112*, 12168.
(42) Zhu, M.; Eckenhoff, W. T.; Pintauer, T.; Jin, R. *J. Phys. Chem. C* **2008**, *112*, 14221.
(43) Heaven, M. W.; Dass, A.; White, P. S.; Holt, K. M.; Murray, R. W. *J. Am. Chem. Soc.* **2008**, *130*, 3754.
(44) Akola, J.; Walter, M.; Whetten, R. L.; Hakkinen, H.; Gronbeck, H. *J. Am. Chem. Soc.* **2008**, *130*, 3756.
(45) Iwasa, T.; Nobusada, K. *J. Phys. Chem. C* **2007**, *111*, 45.

in any structural differences in the $Au_{25}(SG)_{18}$ cluster compared to $Au_{25}(SCH_2CH_2Ph)_{18}$ clusters. The ligand-caused structural differences have previously been reported in gold phosphine clusters.[46]

In this work, we employ nuclear magnetic resonance (NMR) spectroscopy in combination with laser desorption ionization mass spectrometry (LDI-MS) and optical spectroscopy to probe the structure and charge state of the $Au_{25}(SG)_{18}$ clusters. NMR is particularly useful in identifying the binding modes of surface thiolate ligands, while MS provides insightful information on the metal core structure by studying its fragmentation behavior. On the basis of detailed NMR, MS, and optical spectroscopic analyses, we confirm that the $Au_{25}(SG)_{18}$ cluster indeed adopts the same structure as that of $Au_{25}(SCH_2CH_2Ph)_{18}$ and that the native $Au_{25}(SG)_{18}$ cluster bears one negative charge. The intriguing chiroptical activity observed in $Au_{25}(SG)_{18}$ clusters seems to be imparted by the chiral glutathione ligands because no similar chiroptical signals were observed in $Au_{25}(SCH_2CH_2Ph)_{18}$.

2. Experimental Section

Chemicals. Tetrachloroauric (III) acid ($HAuCl_4 \cdot 3H_2O$, >99.99% metals basis, Aldrich), tetraoctylammonium bromide (TOAB, ≥98%, Fluka), L-glutathione, reduced (≥99%, Aldrich), 2-phenylethanethiol (99%, Acros Organics), 1-hexanethiol (96%, Acros Organics), 1-dodecanethiol (98%, Acros Organics), tetrahydrofuran (THF, HPLC grade, ≥ 99.9%, Aldrich), methanol (HPLC grade, ≥ 99.9%, Aldrich), toluene (HPLC grade, ≥99.9%, Aldrich), acetonitrile (HPLC grade, ≥99.9%, Acros Organics), ethanol (absolute, 200 proof, Pharmco), methylene chloride (HPLC grade, ≥ 99.9%, Aldrich), and hexane (HPLC grade, ≥ 95%, Aldrich). All chemicals were used as received except THF was bubbled with N_2 in experiments. Nanopure water (resistivity: 18.2 MΩ·cm) was produced with a Barnstead NANOpure water system. All glassware was thoroughly cleaned with aqua regia (HCl/HNO_3 = 3:1 vol), rinsed with copious Nanopure water, and then oven-dried prior to use.

Synthesis of $Au_{25}(SR)_{18}$ Clusters. The $Au_{25}(SG)_{18}$ clusters were synthesized following a one-pot method.[33] The $Au_{25}(SCH_2CH_2Ph)_{18}$ clusters were synthesized following a kinetically controlled synthetic method reported in our previous work.[32a]

The $Au_{25}(SC_6H_{13})_{18}$ and $Au_{18}(SC_{12}H_{25})_{18}$ clusters were prepared as follws. Briefly, a toluene solution (2.5 mL) of TOABr (0.11 mmol) was added to an aqueous solution (1.3 mL) of $HAuCl_4$ (0.1 mmol). After magnetic stirring for ~15 min, phase transfer was completed, and the aqueous layer was then removed. The remaining toluene solution was cooled to ~0 °C in an ice bath over a period of 30 min. *n*-$C_6H_{13}SH$ (0.5 mmol) or *n*-$C_{12}H_{25}SH$ (0.5 mmol) was added, and the solution was slowly stirred for ~2 h until the solution became clear. A freshly made, aqueous solution of $NaBH_4$ (1 mmol, dissolved in 1.3 mL of ice-cold nanopure H_2O) was then added rapidly into the reaction mixture under vigorous stirring. After 3 h of reaction, the ice-bath was removed, and the solution was continuously stirred for over 24 h (in our previous work,[33] we found the aging time markedly influences the purity and yield of $Au_{25}(SR)_{18}$ clusters). The postsynthesis was done as follows: the organic phase was evaporated to dryness, and the product was washed twice with methanol to remove excess $C_6H_{13}SH$ or $C_{12}H_{25}SH$. The $Au_{25}(SC_6H_{13})_{18}$ clusters were extracted from the dried product with pure acetonitrile, and subsequently with 1:1 acetonitrile/acetone, while the $Au_{25}(SC_{12}H_{25})_{18}$ clusters were extracted from the dried product with pure acetone repeatedly.

Characterization. All UV−vis absorption spectra were recorded in the range of 190−1100 nm using a Hewlett-Packard (HP) 8543 diode array spectrophotometer. Laser desorption ionization (i.e., no matrix) mass spectrometry analyses were performed with a PerSeptive Biosystems Voyager DE super-STR time-of-flight (TOF) mass spectrometer. Nuclear magnetic resonance (NMR) analysis was conducted on a Bruker Avance DMX 500 spectrometer operating at 500.13 MHz for ^1H and 125.77 MHz for ^{13}C, using standard Bruker software. The data were collected with samples dissolved in D_2O (for $Au_{25}(SG)_{18}$ clusters). The NMR assignments were made using the following experiments: 1D ^1H NMR, $^1H-^1H$ correlation spectroscopy (COSY), and $^1H-^{13}C$ heteronuclar single quantum correlation spectroscopy (HSQC). Transmission electron microscopy (TEM) images of $Au_{25}(SG)_{18}$ clusters were obtained on a Hitachi 7000 TEM operated at 75 kV. For circular dichroism (CD) measurements, $Au_{25}(SG)_{18}$ and $Au_{25}(SCH_2CH_2Ph)_{18}$ clusters were dissolved in water and CH_2Cl_2, respectively, in 1-cm path-length quartz cuvettes. CD spectra were recorded at 22 °C on a Jasco J-715 spectropolarimeter.

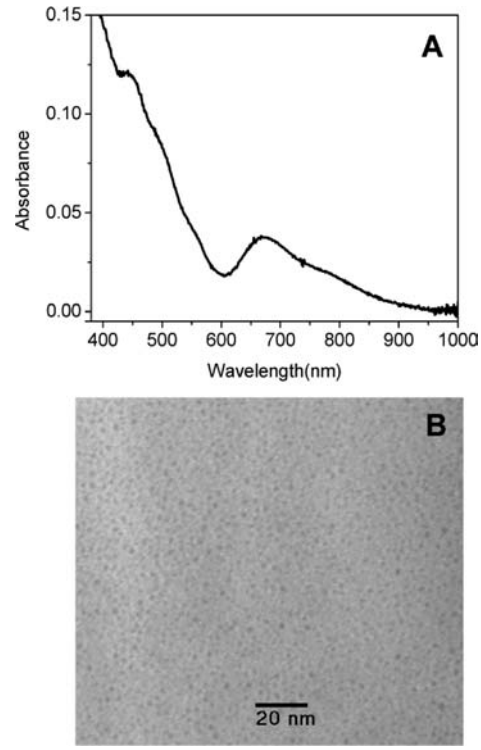

Figure 1. The optical absorption spectrum (A) and TEM image (B) of $Au_{25}(SG)_{18}$ clusters.

3. Results and Discussion

The glutathione-capped $Au_{25}(SG)_{18}$ clusters synthesized by the one-pot method[33] show a well-defined optical absorption spectrum characteristic of thiol-capped Au_{25} nanoclusters (Figure 1A). Three peaks at ~670, 450, and 400 nm are observed and are similar to phenylethylthiolate-capped Au_{25} clusters. These spectral features might indicate that the two types of Au_{25} clusters share a common structure. TEM showed that the average cluster size is about ~1 nm (Figure 1B), note that the image contrast is quite low due to the extremely small size of Au_{25} clusters.

Below we shall present NMR and mass spectrometry analyses of $Au_{25}(SG)_{18}$ clusters and rationalize its core structure, surface ligand distribution, and the charge state.

3.1. NMR Analysis of $Au_{25}(SG)_{18}$ Clusters. The ^1H NMR spectrum of $Au_{25}(SG)_{18}$ clusters is shown in Figure 2A. The proton peaks in the range of 2.0 to ~4.8 ppm; note that the

(46) (a) Mingos, D. M. P. *Polyhedron* **1984**, *3*, 1289. (b) Mingos, D. M. P. *J. Organomet. Chem.* **1995**, *500*, 251. (c) Stefanescu, D.; Glueck, D.; Siegel, R.; Wasylishen, R. *Langmuir* **2004**, *20*, 10379.

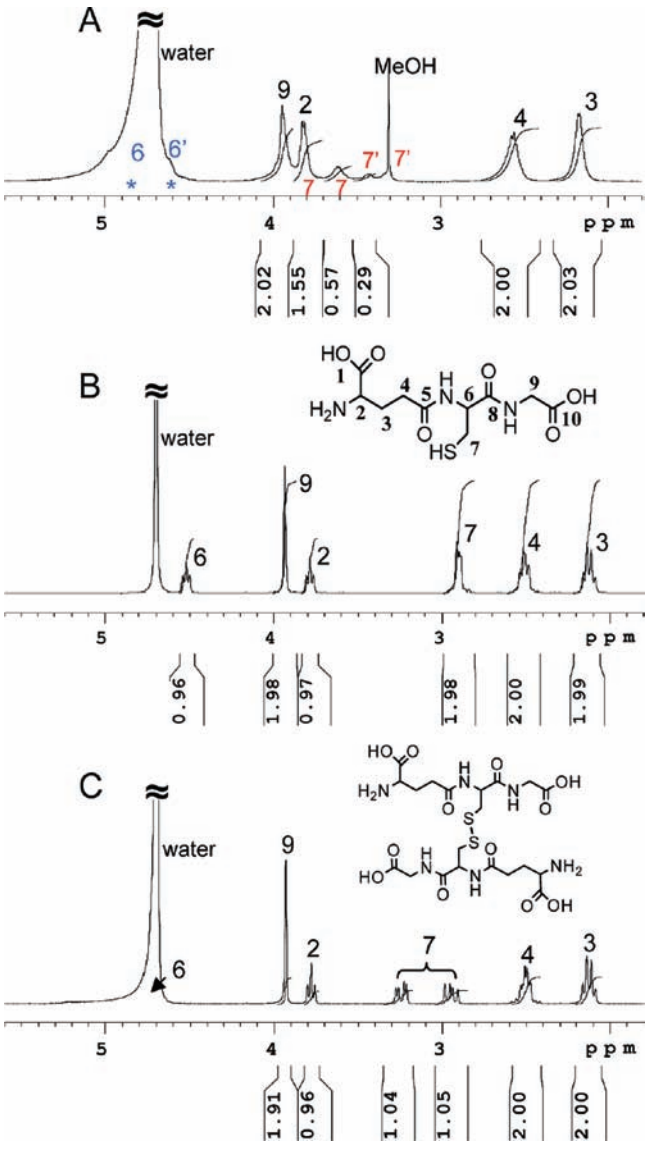

Figure 2. NMR spectra of $Au_{25}(SG)_{18}$ clusters (A), free GSH (B), and disulfide GS-SG (C). Solvent: D_2O. The numbers 1−10 label the carbon atoms in GSH, see inset in (B).

strong peak at 4.75 ppm arises from residual H_2O in the sample and HDO in D_2O NMR solvent. All the peaks of $Au_{25}(SG)_{18}$ are significantly broadened compared to the case of free GSH (Figure 2B); thus, the assignment of the 1D spectrum is quite difficult due to the loss of *J*-coupling information, and some of the peaks are indeed ambiguous if solely based upon the 1D spectral information.

To attain an unambiguous assignment, we start with the assignment of pure GSH and use the chemical shift information to aid peak assignment for $Au_{25}(SG)_{18}$. For convenience, the carbon atoms in GSH are labeled with numbers 1−10 (Figure 2B, inset). The strong singlet at 3.92 ppm (Figure 2B) is readily assigned to the CH_2 at C-9 since it does not couple to other H's, and the multiplet at 2.12 ppm is apparently from the CH_2 at C-3 since this is the only one that couples to two hydrogen groups and gives rise to a multiplet. For other protons, by checking the *J*-coupling constants and integrated peak areas (Figure 2B), it is quite straightforward to fully assign the ^1H peaks of pure GSH (see peak labels in Figure 2B); note that the carbon atoms C-1, C-5, C-8, and C-10 do not bear hydrogen. It should be noted that in previous work,[25b,39a,41] there were some incorrect assignments of the NMR peaks of GSH.

On the basis of the chemical shifts of pure GSH, one can readily assign the signals of protons H-2, H-3, H-4, and H-9 of glutathionate in $Au_{25}(SG)_{18}$ since their chemical shifts are not significantly shifted, Figure 2A. These assignments are also confirmed by 2D correlation spectra (*vide infra*). Protons H-6 and H-7 (i.e., the β-CH and α-CH_2 *relative to* the thiol group), however, become quite complicated and cannot be simply assigned based solely upon the 1D spectral information. Note that the sharp peak residing on the broad peak at $\delta \sim 3.3$ ppm is from residual MeOH solvent (^1H NMR: 3.3 ppm, ^{13}C NMR: 49.5 ppm) in our sample. Since protons H-7 (α-CH_2) and H-6 (β-CH) are both very close to the gold core, it is likely that these proton signals significantly downfield shift, and the H-6 (β-CH) signal possibly merges with the strong water peak at ~4.7 ppm (this is indeed the case, *vide infra*). In addition, the set of broad peaks in the range of 3.2−3.8 ppm need careful assignments. Herein, we introduce 2D correlation NMR spectroscopy, including heteronuclear single quantum correlation (HSQC) and homonuclear correlation spectroscopy (COSY), to aid peak assignment and extract detailed information on the thiolate ligand distribution on the $Au_{25}(SG)_{18}$ cluster surface.

The HSQC experiment was collected in edited mode, where the one-bond $^1H-^{13}C$ cross-correlation peaks show positive phase (in black) for CH and CH_3 groups and negative phase (in red) for CH_2 groups, Figure 3A. The COSY spectrum reveals *J*-coupled (through bond) hydrogen groups via cross-correlation peaks off the diagonal, Figure 3B. Below we utilize both HSQC and COSY spectral information to attain full peak assignments of $Au_{25}(SG)_{18}$ clusters.

In the HSQC, the peaks at 2.2 and 2.6 ppm are CH_2 signals (in red, Figure 3A) connected to two different carbon atoms (27 ppm and 32 ppm, see the ^{13}C dimension) and are *J*-correlated because of the presence of a cross peak in the COSY spectrum (Figure 3B). Therefore, these two signals must correspond to protons H-3 and H-4 since they are the only pair in the glutathione structure, confirming the aforementioned 1D spectral assignment (Figure 2A).

The peaks at 3.3 and 3.4 ppm are also CH_2 signals (in red) but connect to the *same* carbon (~34.5 ppm, Figure 3A) and are *J*-coupled (Figure 3B). Similarly, HSQC and COSY spectra reveal another pair of *J*-coupled CH_2 at 3.6 and 3.8 ppm that are bonded to the same carbon (~38 ppm). These two pairs are assigned to the protons at C-7, labeled as H-**7** and H-**7′**, respectively (Figure 3 and Figure 2A). The signal splitting of the 3.3/3.4 (ppm) pair as well as the 3.6/3.8 (ppm) pair is caused by the nearby chiral carbon (C-6, see Figure 2B inset). Such a chirality-induced peak splitting is also observed in the ^1H spectrum of disulfide (GS-SG, Figure 2C): the protons at C-7 are split into two groups at 2.95 and 3.23 ppm, respectively, and the split ^1H signals at C-6 merge with the water peak (Figure 2C) and, hence, are not observed.

Note that the 3.8 ppm peak also contains a C**H** signal (in black, Figure 3A) from C-2 (^{13}C: ~54.5 ppm), which is correlated with CH_2 at C-3 (see the cross peak in the COSY plot, Figure 3B). Therefore, the 3.8 ppm peak in the 1D spectrum is composed of two overlapped signals from proton H-2 (^{13}C peak at 54.5 ppm) and H-**7** (^{13}C peak at 38 ppm). The sum of integrals of H-**7** and H-**7′** in the 1D NMR spectrum ($0.57 \times 2 + 0.29 \times 2 = 1.72$) roughly corresponds to two protons.

Surprisingly, both COSY and HSQC (Figure 3A and B) reveal that, under the water peak (~4.7 ppm), there are two CH groups

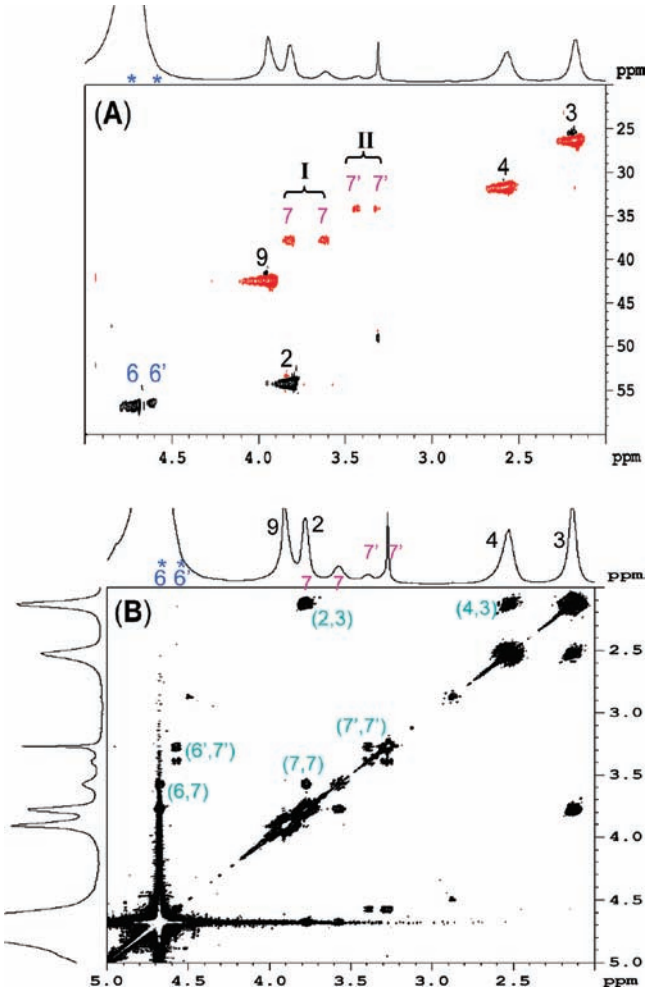

Figure 3. 2D NMR spectra of $Au_{25}(SG)_{18}$ clusters. (A) Edited mode HSQC spectrum (red: CH_2, black: CH or CH_3). (B) COSY spectrum. Solvent: D_2O. Note that the CH_3 signal (^1H: 3.3 ppm, ^{13}C: 49.5 ppm) in the HSQC spectrum is from residual CH_3OH in our sample; the signal splitting in [7, 7] as well as in [7′, 7′] is caused by the chiral C-6 in glutathionate.

at 4.60 ppm and 4.75 ppm, respectively. These two signals are coupled to H-**7** and H-**7′**, respectively (Figure 3B). Therefore, these two signals must correspond to the β-CH protons at C-6 that were missing in the 1D spectrum (Figure 2A); for the convenience of discussion, these two signals are labeled as H-**6** and H-**6′**, respectively.

Thus far, we have unambiguously assigned all the NMR peaks of $Au_{25}(SG)_{18}$ clusters with the aid of 2D correlation spectra. Below we proceed to unravel the structure of $Au_{25}(SG)_{18}$ clusters.

3.2. Probing the Chemical Environments of Thiolate Ligands on $Au_{25}(SG)_{18}$ Clusters. More information can be extracted by looking into the splitting behavior of the α-CH_2 (marked as **7** and **7′**). The α-CH_2 is quite informative as it is the closest to the Au_{25} core and can thus "sense" the gold core, e.g., the electronic state of the metal core; for example, any charge transfer effect would directly influence the chemical shift of the α-CH_2. Excluding the chirality-induced splitting (e.g., in the pair [7, 7]), the four peaks (pairs of [7, 7] and [7′, 7′] in the 3.3−3.8 ppm range indicate that there are two types of chemically distinct thiolate-gold binding modes, which is indeed in agreement with the recently determined crystal structure of $Au_{25}(SCH_2CH_2Ph)_{18}$ clusters.[1,43] The structure of the $Au_{25}(SCH_2CH_2Ph)_{18}$ cluster is based on a centered icosahedral Au_{13} kernel; the kernel is further capped by a second gold shell composed of the remaining 12 Au atoms (Scheme 1), hence, a two-shell structure. The entire Au_{25} core is encapsulated by 18 phenylethylthiolates. In another view, the cluster can be regarded as an icosahedral Au_{13} kernel capped by six "staple" motifs (−S−Au−S−Au−S−) in the *x*, *y*, and *z* directions, Scheme 1A. Overall, the $Au_{25}(SCH_2CH_2Ph)_{18}$ structure shows two types of chemically distinct thiolate−Au binding modes with different bonding lengths and angles (Scheme 1B), (i) the interior Au−S−Au mode I (a total of 12 such −SR ligands), these thiolate ligands connect the icosahedron and the exterior gold shell, and (ii) the V-shaped Au−S−Au mode II (a total of six such ligands), which connect each pair of exterior gold atoms (total six pairs). The ratio of the number of ligands in mode I to that in II is 2:1. The Au−S bond length in mode I is ∼2.35 Å (bond angle of ∼86°), while the bond length in mode II is somewhat shorter ∼2.30 Å (larger bond angle ∼102°). Apparently, these two binding modes will result in differences in the chemical shifts of the α-CH_2 and β-CH protons in the thiolate ligands.

Scheme 1. Structure of $Au_{25}(SCH_2CH_2Ph)_{18}$ Clusters: (A) Overall Structure of the Cluster (For Clarity, the $-CH_2CH_2Ph$ Moiety Is Not Shown); (B) Portion of the Structure along the *z*-Direction; the Au_{13} Kernel Is Capped by a Second Au_{12} Shell, and the Entire Cluster Is Encapsulated by 18 Thiolates: Purple: Au Atoms; Yellow: S Atoms

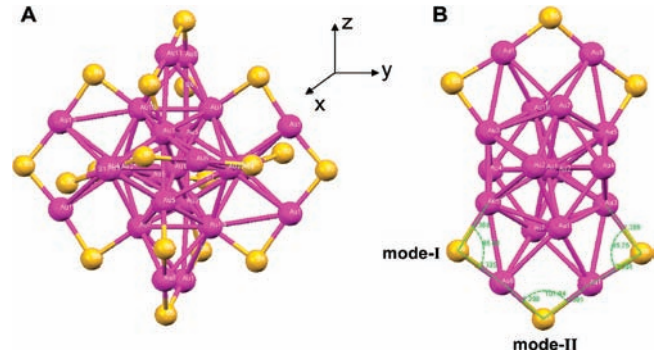

Interestingly, the ratio of the two binding modes observed in the NMR analysis of $Au_{25}(SG)_{18}$ clusters is exactly 2:1 (peak area of H-**7**:H-**7′** = 0.57:0.29 = 2: 1, Figure 2A), which is quantitatively in agreement with the crystal structure of $Au_{25}(SCH_2CH_2Ph)_{18}$ clusters. This result indicates that the $Au_{25}(SG)_{18}$ clusters might adopt a two-shell structure similar to that of $Au_{25}(SCH_2CH_2Ph)_{18}$, Scheme 1. Additional information about the ligand environments can be inferred from the NMR spectrum of $Au_{25}(SG)_{18}$ clusters (Figures 2A and 3A), the α-CH_2 corresponding to mode-I (marked as **7**) markedly shifts toward downfield (3.6/3.8 ppm in the cluster compared to 2.9 ppm in free GSH), Figure 2A and B. This shift is larger than that of mode-II α-CH_2 (marked as **7′**, 3.3/3.4 ppm in the cluster compared to 2.9 ppm in free GSH). This difference in chemical shifts of α-CH_2 (**7** and **7′**) in the two binding modes (I and II) can be understood by the following argument. The sulfur in mode-I (which joins the interior Au_{13} icosahedron and exterior gold atoms, Scheme 1B) is more strongly influenced by the electronic properties of the Au_{13} kernel, while the sulfur in mode-II (locating at the exterior) is less influenced by the Au_{13} kernel since the ligand is relatively isolated from the Au_{13} kernel due to the shielding effect by the exterior gold shell (Au_{12}). In other words, the ligand in mode-I would experience a stronger electronic induction effect, which leads to a larger downfield shift of the α-CH_2 in the −SG ligand.

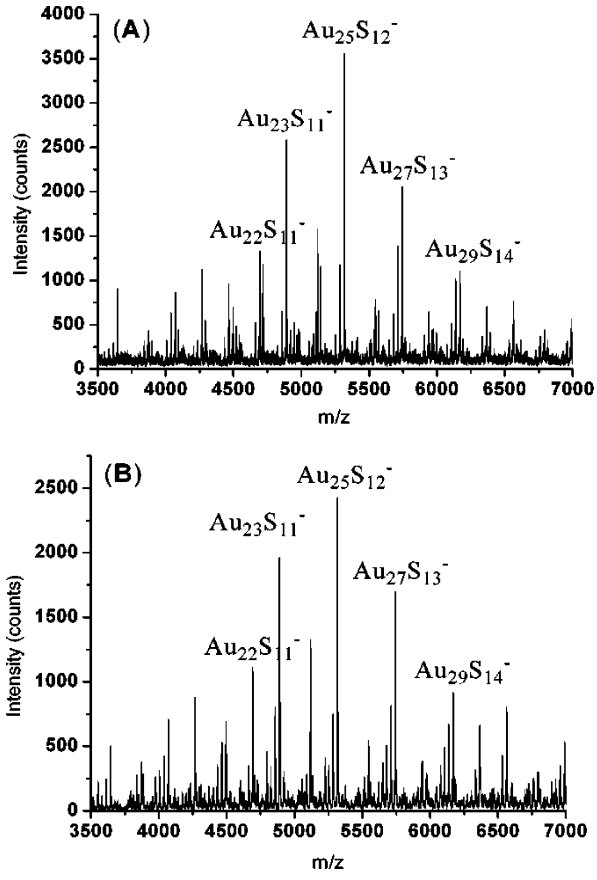

Figure 4. Laser desorption ionization (LDI) mass spectra of $Au_{25}(SG)_{18}$ (A) and $Au_{25}(SCH_2CH_2Ph)_{18}$ (B). Both spectra were collected in the negative ion mode.

A similar effect on the splitting of the β-CH (marked as **6** and **6′**) was also observed, which is caused by the two different binding modes (Figure 3A). Although one cannot accurately calculate the ratio of the peak areas of H-**6** and H-**6′** because they are overlapped with the strong water peak ($\delta \sim 4.7$ ppm), we roughly estimated the ratio of H-**6** to H-**6′** by integrating the *volumes* of the peaks in the 2D HSQC spectrum (Figure 3A), which gives rise to a ratio of roughly 2:1; therefore, protons H-**6** and H-**6′** correspond to mode-I and mode-II, respectively, similar to the case of H-**7** and H-**7′**.

Taken together, the NMR analysis of $Au_{25}(SG)_{18}$ clusters indicates that the surface $-$SG ligands in $Au_{25}(SG)_{18}$ exhibit two different chemical environments with a ratio of 2:1 (the ratio of low-field protons to high-field protons). These results are consistent with the ligand distribution revealed by the crystal structure of $Au_{25}(CH_2CH_2Ph)_{18}$ clusters. Thus, the $Au_{25}(SG)_{18}$ cluster should adopt the same two-shell structure as that of $Au_{25}(SCH_2CH_2Ph)_{18}$.

3.3. Further Evidence from Mass Spectrometry Analysis of $Au_{25}(SG)_{18}$. Mass spectrometry analysis provides further strong evidence that $Au_{25}(SG)_{18}$ adopts the same two-shell structure as that of their phenylethylthiolate counterparts. Laser desorption ionization mass spectrometry (LDI-MS, i.e. no matrix added) shows strong signals from the $Au_{25}(SG)_{18}$ clusters when operated in negative-ion mode, Figure 4A. Interestingly, the spectrum is almost identical to that of $Au_{25}(SCH_2CH_2Ph)_{18}$ under the same LDI conditions, Figure 4A and B. The most abundant peak is centered at 5308 *m/z*, and the low-mass and high-mass sides of the 5308 *m/z* peak show a series of fragments and recombined ion peaks in both types of Au_{25} clusters.

By checking the high-resolution pattern of the 5308 *m/z* peak (collected in the reflectron negative mode, data not shown), we found that the gaseous ion bears -1 charge (evidenced by the unity spacings of the high-resolution peaks in the isotopic pattern); thus, the actual mass of the *m/z* 5308 ion is $5308 \times 1 = 5308$ Da, which corresponds to that of $Au_{25}S_{12}$ (also confirmed by the excellent agreement of the isotopic pattern with simulation[32a]). Note that six sulfurs were lost in the $[Au_{25}S_{12}]^-$ ion, presumably via the process $[Au_{25}(SR)_{18}]^- \rightarrow [Au_{25}S_{12}]^- + 6S + 18R$, where, S and R are charge neutral fragments, evidenced by the 32 Da spacing observed in the LDI spectrum (Figure 4). The six lost sulfur atoms are most probably those in the V-shaped Au$-$S$-$Au staples (mode II) since their loss perhaps does not affect the integrity of the Au_{25} core, see Scheme 1.

The LDI process is apparently very complex,[47] and we do not intend to interpret the detailed gas phase fragmentation and recombination processes. Nevertheless, the essentially identical LDI-MS spectra of $Au_{25}(GS)_{18}$ and $Au_{25}(SCH_2CH_2Ph)_{18}$ strongly support that these two clusters share a common two-shell structure as shown in Scheme 1.

3.4. The Possibility of Other Structures for $Au_{25}(SG)_{18}$ Clusters. It is noteworthy that previously Iwasa et al. performed density functional theory (DFT) calculations and predicted two low-energy Au_{25} structures, i.e., face-centered-cubic (fcc) and biicosahedral structures.[45] By checking the chemical environments of the thiolate ligands in these two predicted structures, one can rule out the biicosahedral one because it would have at least three types of thiolate binding modes, but experimentally we only observe two types in $Au_{25}(SG)_{18}$ (excluding the chirality induced peak splitting in glutathionate). In addition, the calculated optical absorption spectrum and XRD pattern for the biicosahedral $Au_{25}(SR)_{18}$ structure do not match experimental data: the predicted absorption band at $\sim$670 nm seems consistent with the two-shell structure, but the short-wavelength peaks at 400 and 450 nm are not predicted. Thus, the possibility of biicosahedral $Au_{25}(SG)_{18}$ structure is ruled out. As for the fcc structure, at first glance it seems possible based upon the UV$-$vis and XRD results since the fcc structure also shows two types of Au$-$S binding modes. But careful scrutiny of the ratio of the two binding modes gives rise to a ratio of 1:2 (the ratio of low-field protons to high-field protons), rather than 2:1 for the two-shell structure (the ratio of low-field protons [7,7] to high-field protons [7′, 7′], see above NMR analyses).

Additional evidence for the two-shell $Au_{25}(SG)_{18}$ structure comes from the recent DFT calculations based upon the crystal structures of $Au_{25}(SCH_2CH_2Ph)_{18}$.[1,2,6] DFT calculations correctly predicted the three peaks at 400, 450, and 670 nm. Therefore, the close resemblance of the optical absorption spectra of $Au_{25}(SG)_{18}$ and $Au_{25}(SCH_2CH_2Ph)_{18}$ strongly indicates that these two clusters share a common two-shell Au_{13}/Au_{12} structure.

3.5. The Charge State of $Au_{25}(SG)_{18}$ Clusters. The afore-discussed NMR, MS, and UV$-$vis data explicitly demonstrate that $Au_{25}(SG)_{18}$ should adopt the same structure as that of $Au_{25}(SCH_2CH_2Ph)_{18}$. Herein, we further investigate the charge state of the as-prepared $Au_{25}(SG)_{18}$ clusters.

In general, it is nontrivial to determine the charge state of clusters. Those conventional methods such as electrochemistry, mass spectrometry, and NMR are all incapable of determining the charge state of clusters. In the case of $Au_{25}(SCH_2CH_2Ph)_{18}$,

(47) (a) Arnold, R. J.; Reilly, J. P. *J. Am. Chem. Soc.* **1998**, *120*, 1528. (b) Schaaff, T. G. *Anal. Chem.* **2004**, *76*, 6187.

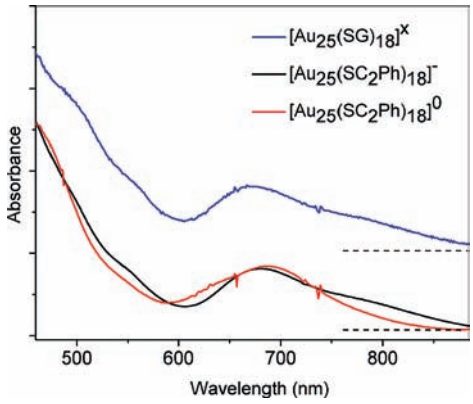

Figure 5. Comparison of the optical absorption spectrum of $Au_{25}(SG)_{18}$ with those of anionic and neutral $Au_{25}(SCH_2CH_2Ph)_{18}$ clusters, respectively. The dashed lines show the baselines.

previously Murray and co-workers identified several charge states in electrochemical analysis by assuming the native charge state of $Au_{25}(SCH_2CH_2Ph)_{18}$ to be zero[48] (but later revealed to be -1 by X-ray crystallographic analysis[1,43]). The charge states of $[Au_{25}(SC_6H_{13})_{18}]^q$ ($q = -1, 0, +1$) were also discussed by Tsukuda and co-workers on the basis of their detailed ESI-MS analysis.[49] Recently, we have been able to isolate and grow single crystals of $[Au_{25}(SCH_2CH_2Ph)_{18}]^0$ clusters. X-ray crystallography showed that the $[Au_{25}(SCH_2CH_2Ph)_{18}]^0$ cluster has an almost identical structure to the anion except some small structural differences;[42] for example, the slight structural distortions (deviated from the $D_{2\,h}$ symmetry) in the anionic $[Au_{25}(SCH_2CH_2Ph)_{18}]^-$ cluster[1] were not observed in the charge neutral $[Au_{25}(SCH_2CH_2Ph)_{18}]^0$ cluster.[42]

For the $Au_{25}(SG)_{18}$ clusters, since their phenylethylthiolate counterparts are already known, to determine the charge state of $Au_{25}(SG)_{18}$ becomes relatively easier with the aid of the known NMR and optical absorption spectral information for the anionic and neutral $Au_{25}(SCH_2CH_2Ph)_{18}$ clusters.[1,42] First of all, the NMR spectra of the anionic and neutral $Au_{25}(SCH_2CH_2Ph)_{18}$ clusters show distinct differences:[42] both the α- and β-CH_2 protons of the $-SCH_2CH_2Ph$ ligand show a much larger downfield shift ($\Delta\delta$, relative to free HS-CH_2CH_2Ph) in the neutral $[Au_{25}(SCH_2CH_2Ph)_{18}]^0$ cluster than in the anionic cluster $[Au_{25}(SCH_2CH_2Ph)_{18}]^-$ (counterion: tetraoctylammonium, TOA^+). On the basis of this information, we compared the NMR spectrum of the native $Au_{25}(SG)_{18}$ with those of $[Au_{25}(SCH_2CH_2Ph)_{18}]^-$ and $[Au_{25}(SCH_2CH_2Ph)_{18}]^0$, respectively, and found that the shift ($\Delta\delta$ ~0.6 ppm) of α-CH_2 of glutathionate in $Au_{25}(SG)_{18}$ is closer to the shift value ($\Delta\delta$ ~0.4 ppm) observed in the anionic $[Au_{25}(SCH_2CH_2Ph)_{18}]^-$ cluster; note that the $\Delta\delta$ value for the neutral $[Au_{25}(SCH_2CH_2Ph)_{18}]^0$ is much larger ($\Delta\delta$ ~2.1 ppm).[42] Therefore, the charge state of native $Au_{25}(SG)_{18}$ clusters should be -1.

The UV−vis spectrum (Figure 5) also provides another evidence for the anionic nature of native $Au_{25}(SG)_{18}$ clusters. In the case of $Au_{25}(SCH_2CH_2Ph)_{18}$, our previous work has determined the crystal structure of the neutral $Au_{25}(SCH_2CH_2Ph)_{18}$ clusters and revealed the spectral differences between the anion and neutral clusters, that is, the anion shows a distinct, broad shoulder at ~800 nm (spin-forbidden transition), while the neutral cluster does not.[42] By comparing the spectrum of native $Au_{25}(SG)_{18}$ clusters with that of the anionic and neutral $Au_{25}(SCH_2CH_2Ph)_{18}$ cluster, Figure 5, it is clear that native $Au_{25}(SG)_{18}$ clusters are indeed anionic since the clusters show a distinct broadband at ~800 nm. The two spectra of $Au_{25}(SG)_{18}$ and $[Au_{25}(SCH_2CH_2Ph)_{18}]^-$ clusters are almost superimposable (including those fine spectral features, such as the broad hump at ~550 nm). This strongly indicates that they possess the same structure and charge state.

Mass spectrometry analysis provides some further evidence (see Supporting Information, Figure S1). In the negative ion mode, we observed strong signals (centered at *m*/*z* 5308) from laser desorption ionization of both $Au_{25}(SG)_{18}$ and $[Au_{25}(SCH_2CH_2Ph)_{18}]^-$ clusters, while in the positive ion mode, no signals centered at *m*/*z* 5308 from both clusters was observed. Herein, an interesting observation is that the core charge state of the $[Au_{25}(SCH_2CH_2Ph)_{18}]^-$ cluster (counterion: TOA+) seems retained in the laser desorption ionization process. The 337 nm laser irradiation selectively breaks up the S−C bond in the ligands,[47] i.e., $[Au_{25}(S\text{-}CH_2CH_2Ph)_{18}]^- \rightarrow [Au_{25}S_{12}]^-$.

Taken together, the -1 charge state of native $Au_{25}(SG)_{18}$ clusters is unambiguous. The counterion for $[Au_{25}(SG)_{18}]^-$ is presumably Na^+, evidenced by the observation of cluster-sodium adducts in the LDI spectrum of pure $Au_{25}(SG)_{18}$ clusters.

3.6. Effect of Thiolate Types and Chain Length on the Au_{25} Core Structure. The above NMR, LDI-MS, and optical spectroscopic analyses all confirm that the $Au_{25}(SG)_{18}$ cluster adopts the same structure as that of their phenylethylthiolate counterparts. Herein, an interesting question arises naturally, that is, whether all 25-atom gold thiolate clusters, regardless of the types of thiols (e.g., long-chain alkylthiols, aromatic thiols, or other functionalized ones), adopt the same two-shell structure (Scheme 1). In previous work of gold phosphine clusters, it has been demonstrated that the size (bulkiness or chain length) of phosphine ligands have a dramatic effect on the structure of gold phosphine clusters.[46]

To answer the major question of whether different types of thiolate ligands result in structural differences in gold clusters, we chose Au_{25} capped by long-chain alkanethiols with different chain lengths (hexylthiol and dodecanethiol) and performed LDI-MS analyses. Interestingly, LDI-MS analyses demonstrate that both $Au_{25}(SC_6H_{13})_{18}$ and $Au_{25}(SC_{12}H_{25})_{18}$ clusters show essentially identical LDI patterns (Supporting Information, Figure S2) with that of $[Au_{25}(SCH_2CH_2Ph)_{18}]^-$, indicating that all these thiolate-capped Au_{25} clusters share the common two-shell structure (see Scheme 1). This observation confirms that in the case of gold thiolate clusters, the types of ligands have very little effect on the cluster structure. The Au_{25} clusters capped by very bulky glutathionate or by much less bulky hexylthiolate have an identical core structure (i.e., two-shell Au_{25}) and charge state (i.e., $q = -1$) based upon the LDI pattern (Supporting Information, Figure S2) and the absorption spectra(Supporting Information, Figure S3).

The fact that different thiols lead to the same Au_{25} core structure indicates the particular stability of the two-shell structure adopted by Au_{25} thiolate clusters. In contrast to gold phosphine clusters, thiolate ligand exchange does not lead to cluster size change.[50] The structural stability of gold thiolate clusters seems to be largely dictated by the electronic effect rather than by any geometric effect (e.g., the bulkiness of thiolate

(48) Lee, D.; Donkers, R. L.; Wang, G.; Harper, A. S.; Murray, R. W. *J. Am. Chem. Soc.* **2004**, *126*, 6193.
(49) Negishi, Y.; Chaki, N. K.; Shichibu, Y.; Whetten, R. L.; Tsukuda, T. *J. Am. Chem. Soc.* **2007**, *129*, 11322.
(50) Dass, A.; Stevenson, A.; Dubay, G. R.; Tracy, J. B.; Murray, R. W. *J. Am. Chem. Soc.* **2008**, *130*, 5940.

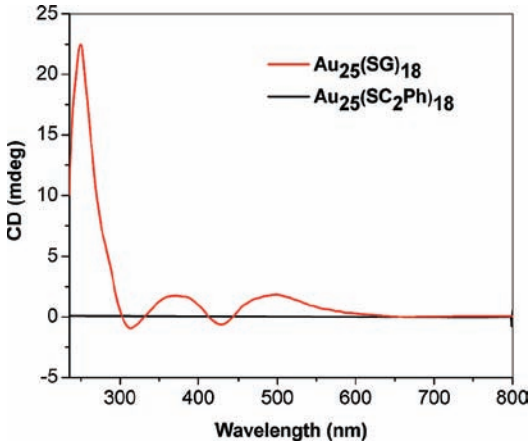

Figure 6. CD spectra of glutathione and phenylethylthiolate-capped Au_{25} clusters. Note that no chiroptical responses were observed from $Au_{25}(SCH_2CH_2Ph)_{18}$.

ligands). Häkkinen et al. recently discussed the applicability of the superatom concept (which was originally proposed to account for the stability of gas phase, bare metal cluster) to ligand-protected gold clusters.[51] Within this picture, the preferred charge state ($q = -1$) of native $[Au_{25}(SR)_{18}]^q$ clusters seems dictated by the electronic shell closing ($1S^21P^6$). However, the stability of different charge states of $Au_{25}(SR)_{18}$ clusters is quite interesting because the $q = 0$ state, which possesses 7e ($1S^21P^5$), rather than a closed electronic shell, is also very stable.[6,42]

3.7. Chiroptical Activity of $Au_{25}(SG)_{18}$ Clusters. The chiral optical responses from the $Au_{25}(SG)_{18}$ clusters is an intriguing issue. It was first observed by Whetten and co-workers.[39] They suggested three possible mechanisms to interpret the origin of the observed optical activity, (i) the structure of the Au_{25} core is inherently chiral; (ii) the adsorption of the −SG thiolates on the core's surface results in a chiral pattern of adsorbate interactions with an inherently achiral core; (iii) chiral elements of the −SG adsorbates induce optical activity in the core electronic structure, even though neither the adsorption pattern nor the core structure is chiral. In our current work, we observed similar circular dichroism (CD) responses from the $Au_{25}(SG)_{18}$ clusters, but the phenylethylthiolate-capped Au_{25} clusters do not exhibit such chiral optical responses, Figure 6.

The chiroptical signals from $Au_{25}(SG)_{18}$ is apparently not caused by the chiral Au_{25} core since $Au_{25}(SG)_{18}$ and $Au_{25}(SCH_2CH_2Ph)_{18}$ are demonstrated to possess the same structure and the $Au_{25}(SCH_2CH_2Ph)_{18}$ cluster does not show any CD signals. In addition, the NMR spectrum of $Au_{25}(SG)_{18}$ as well as of $Au_{25}(SCH_2CH_2Ph)_{18}$ (including the anionic and neutral clusters[42]) does not show any Au_{25} core chirality-induced peak splitting (excluding the chiral C-6-induced NMR peak splitting in the case of −SG, see Figure 3A). Therefore, the first proposed mechanism of chirality coming from the Au_{25} core can be ruled out. The second mechanism (i.e., chirality coming from the thiolates) can also be ruled out since free glutathione shows a CD signal in the UV (at ∼230 nm) and should not shift to the visible wavelength region. In addition, no chiral adsorption pattern of thiolates was found in the case of $Au_{25}(SCH_2CH_2Ph)_{18}$. Taken together, we deem that the chiroptical responses from the $Au_{25}(SG)_{18}$ cluster are due to the chiral induction of the −SG ligands. Similar effects were also observed in other clusters capped by phosphine or thiolate.[52−54] Nevertheless, a concrete conclusion remains to be made after the crystal structure of $Au_{25}(SG)_{18}$ clusters is solved in the future. Theoretical calculations will also facilitate to clarify this intriguing issue.[55−57]

4. Conclusion

In summary, on the basis of NMR, mass spectrometry and optical spectroscopy analyses we conclude that $Au_{25}(SG)_{18}$ clusters should adopt the same two-shell structure as that of the $Au_{25}(SCH_2CH_2Ph)_{18}$ cluster and that the charge state of the native $Au_{25}(SG)_{18}$ cluster is −1, i.e. $[Au_{25}(SG)_{18}]^-$ (counterion: Na^+). Given the major difficulties encountered in growing high-quality single crystals of gold thiolate nanoclusters (except the case of $Au_{25}(SCH_2CH_2Ph)_{18}$), NMR can be an important and indispensable tool for gaining insight into the structure of gold clusters. We have demonstrated that the complicated 1D ^1H NMR spectrum of $Au_{25}(SG)_{18}$ clusters, with the aid of 2D NMR experiments (COSY and HSQC), can provide a wealth of information on and facilitate identification of the structure of $Au_{25}(SG)_{18}$ clusters when combined with mass spectrometry and optical spectroscopy. Overall, this combined approach, as demonstrated in this work, could be useful and benefit future studies in determining the cluster structure and surface ligand distribution. The conclusion from this work, that is, all $Au_{25}(SR)_{18}$ clusters capped by different types of thiolate ligands investigated in this work (R = G, CH_2CH_2Ph, C_6H_{13}, $C_{12}H_{23}$) should adopt a common two-shell structure, will benefit future studies of this unique Au_{25} cluster material. The two-shell structure of $Au_{25}(SR)_{18}$ clusters not being influenced by thiolate types indicates the particular structural stability of the cluster. The intriguing chiral optical responses from the $Au_{25}(SG)_{18}$ clusters are demonstrated to be imparted by the chiral glutathione ligands, rather than by the chirality of the Au_{25} core.

Acknowledgment. This work is supported by CMU, AFOSR, and PITA. We thank Joseph Suhan for TEM imaging of the $Au_{25}(SG)_{18}$ clusters. The NMR instrumentation at Carnegie Mellon University was partially supported by NSF (CHE-0130903).

Supporting Information Available: The LDI-MS and optical absorption spectra of $Au_{25}(SG)_{18}$, $Au_{25}(SCH_2CH_2Ph)_{18}$, $Au_{25}(SC_6H_{13})_{18}$, and $Au_{25}(SC_{12}H_{25})_{18}$ (Figures S1, S2, and S3). This material is available free of charge via the Internet at http://pubs.acs.org.

JA900386S

(51) Walter, M.; Akola, J.; Lopez-Acevedo, O.; Jadzinsky, P. D.; Calero, G.; Ackerson, C. J.; Whetten, R. L.; Grönbeck, H.; Häkkinen, H. *Proc. Natl. Acad. Sci. U.S.A.* **2008**, *105*, 9157.

(52) Yanagimoto, Y.; Negishi, Y.; Fujihara, H.; Tsukuda, T. *J. Phys. Chem. B* **2006**, *110*, 11611.

(53) (a) Yao, H.; Miki, K.; Nishida, N.; Sasaki, A.; Kimura, K. *J. Am. Chem. Soc.* **2005**, *127*, 15536. (b) Yao, H.; Fukui, T.; Kimura, K. *J. Phys. Chem. C* **2008**, *112*, 16281.

(54) (a) Gautier, C.; Bürgi, T. *J. Am. Chem. Soc.* **2006**, *128*, 11079. (b) Gautier, C.; Burgi, T. *J. Am. Chem. Soc.* **2008**, *130*, 7077.

(55) Román-Velázquez, C. E.; Noguez, C.; Garzón, I. L. *J. Phys. Chem. B* **2003**, *107*, 12035.

(56) Jiang, D.-E.; Dai, S. *Inorg. Chem.* **2009**, *48*, 2720.

(57) Pei, Y.; Gao, Y.; Zeng, X. C. *J. Am. Chem. Soc.* **2008**, *130*, 7830.